Acta Oceanol. Sin., 2022, Vol. 41, No. 3, P. 1–10
https://doi.org/10.1007/s13131-021-1922-z
http://www.aosocean.com
E-mail: ocean2@hyxb.org.cn

Comparison of nominal and standardized catch per unit effort data in quantifying habitat suitability of skipjack tuna in the equatorial Pacific Ocean

Cheng Zhou[1,2], Yuanyuan Hu[1,2], Jie Cao[3], Liuxiong Xu[1,2], Xuefang Wang[1,2*], Rong Wan[1,2], Yu Xiao[1,2], Jiangfeng Zhu[1,2], Hao Tang[1,2]

[1] College of Marine Sciences, Shanghai Ocean University, Shanghai 201306, China

[2] National Engineering Research Center for Oceanic Fisheries, Shanghai 201306, China

[3] Department of Applied Ecology, Center for Marine Sciences and Technology, North Carolina State University, Morehead City, NC 28557, USA

Received 18 December 2020; accepted 11 February 2021

© Chinese Society for Oceanography and Springer-Verlag GmbH Germany, part of Springer Nature 2022

Abstract

In the western and central Pacific Ocean, upper strata waters exhibit highly dynamic oceanographic features under ENSO variability. This has been proved to be responsible for the dynamic change of both abundance and zonal distribution of skipjack tuna (*Katsuwonus pelamis*). Although causality has been suggested by researchers using physical–biological interaction models, cumulative evidence needs to be obtained and the tenability of assertion needs to be tested from an ecological habitat perspective, based on fisheries data. For purse seine fishery, the use of catch per unit effort (CPUE) as an indication of the abundance is confusing because of technical improvements over the whole exploitation history and unbalanced individual fishing characteristic of vessels. It is particularly interesting to discriminate between habitat characteristics in comparative scenarios of CPUE application. This study identified habitat traits based on a series of oceanographic factors from a global ocean reanalysis model. A comparison was conducted between two habitat models based on unprocessed purse seine CPUE and standardized CPUE considering fishing characteristics. The results suggest that standardized CPUE could model the regular zonal shift of habitat compatible with the observed fishing efforts transfer, and achieved better prediction capacity than unprocessed CPUE. Furthermore, the habitat of skipjack tuna was also characterized and linked with surface and subsurface thermal environment, ocean current, dissolved oxygen, biotic environment, and ENSO variability. The monthly-averaged habitat suitable index, derived from the optimal habitat model prediction, showed a significant linear relationship with the southern oscillation index, which suggested that El Niño episodes eventually provide more preferable habitat for skipjack tuna under ENSO variability.

Key words: skipjack tuna, free-swimming schools, habitat characteristics, ENSO events, CPUE standardization

Citation: Zhou Cheng, Hu Yuanyuan, Cao Jie, Xu Liuxiong, Wang Xuefang, Wan Rong, Xiao Yu, Zhu Jiangfeng, Tang Hao. 2022. Comparison of nominal and standardized catch per unit effort data in quantifying habitat suitability of skipjack tuna in the equatorial Pacific Ocean. Acta Oceanologica Sinica, 41(3): 1–10, doi: 10.1007/s13131-021-1922-z

1 Introduction

In the basin of the equatorial Pacific Ocean, waters of upper strata geographically exhibit two polar oceanographic features. One is a strong divergent equatorial upwelling system, which is called the cold tongue in the central and eastern Pacific. This is a zonal band of cold and salty waters, and highly enriched primary production. As its counterpart, the western Pacific shows a prominent warm pool characterized by fresh and oligotrophic waters, which are some of the warmest surface waters (Picaut et al., 1996; Lehodey et al., 1997; Le Borgne et al., 2002). The western Pacific Warm Pool area is considered to be the most productive fishing ground, which contributes to a dominant proportion of global tuna catches. Among these, more than 70% originate from purse seine fisheries that primarily harvest surface-schooling mixtures of skipjack tuna (*Katsuwonus pelamis*) and yellowfin tuna (*Thunnus albacares*).

The convergence zone at the eastern edge of this warm pool is induced by westward advection of the South Equatorial Current (SEC) and has been found to be intimately linked to the distribution of tunas. This dependence could explain why skipjack tuna catches shift under El Niño-Southern Oscillation (ENSO) events (i.e., these shift westward during La Niñas and eastward during El Niños) (Lehodey et al., 1997; Wang et al., 2014; Yen et al., 2017). In terms of the ecological environment, ENSO has been proved to profoundly influence the variability of oceanic stratification, thermal environment, and primary productivity (Lehodey et al., 2013; Matear et al., 2015). More sophisticated causality between ENSO variability and tuna abundance has been inferred by a range of studies that applied physical–biological interaction models. Representative studies used the spatial environmental population dynamic model (SEPODYM) (Bertignac et al., 1998; Loukos et al., 2003; Lehodey et al., 2008) and the apex predator

Foundation item: The National Key R&D Program of China under contract Nos 2020YFD0901202 and 2019YFD0901502; the National Natural Science Foundation of China under contract Nos 41806110, 41506151 and 31902426.

*Corresponding author, E-mail: xfwang@shou.edu.cn

ecosystem model-estimation (APECOSM-E) (Dueri et al., 2014). The results showed that the extension of warm waters in the central Pacific and the increases of primary productivity in the western areas, which can be observed during El Niño events, extend the skipjack spawning grounds and yield higher recruitments to fisheries (Lehodey, 2001; Lehodey et al., 2003). Those models use optimized parameterization to obtain better outputs by adjoining fishing information (e.g., a statistical assimilation process). However, the use of a common statistical approach (e.g., a habitat model of directly fitting to fisheries data) may provide additional proof of population dynamic processes under climatic-oceanographic variability, which may be compatible with the previous understandings.

The physiological and foraging requirements are critical factors driving the spatial distribution of skipjack tuna and contribute to the formation of local high-abundance habitats (Barkley et al., 1978; Brill, 1994; Zainuddin et al., 2006; Schick and Lutcavage, 2009). More recently, tagging experiments have refined the understanding of the physiological adaptation and habitat characteristics of skipjack tuna, revealing that they are restricted to the mixed layer, but make occasional and brief dives below the thermocline due to enhanced thermal inertia of the body (Schaefer and Fuller, 2007; Bernal et al., 2017). In the western Pacific, the 29°C sea surface temperature (SST) isotherm is considered to provide reasonable proxy for the movement of tuna populations (Lehodey et al., 1997). Skipjack tuna are strongly influenced by the ambient surface temperature, which has been repeatedly corroborated by numerous studies as the main environmental factor for interpreting the occurrence and abundance of skipjack tuna in warm waters (Andrade, 2003; Mugo et al., 2010; Yen et al., 2017). Stratifications of the upper ocean by mixed layer and dissolved oxygen were used to define the spatial limits of the skipjack tuna habitat (Barkley et al., 1978; Arrizabalaga et al., 2015). In addition, mesoscale oceanographic features, such as positive/negative sea surface height anomalies, reflect important anticyclonic or cyclonic eddy fields corresponding to convergent and divergent areas. These variables have been coupled with the eddy kinetic energy index to develop the integrated habitat model (Zainuddin et al., 2008; Mugo et al., 2010). In addition, Skipjack tuna are opportunistic feeders of the short food web (Roger, 1994). The concentration of chlorophyll *a*, the main indicators of primary productivity, indirectly influences the abundance of skipjack tuna in a trophic system through the linkage between phytoplankton and prey.

The most commonly used approaches employed by tuna-habitat-related studies include either a simple linking of the raw catch per unit effort (CPUE) with environmental variables (Mugo et al., 2010; Yen et al., 2017), or performing a standardization of raw CPUE for the subsequent analysis (Lan et al., 2018). Although purse seine fisheries accounts for most of the tuna catch, the majority of studies were based on longline and pole-and-line fisheries data. The challenge is that CPUE metrics from purse seine (e.g., catch per set or per day) are likely relatively insensitive to changes in stock abundance (Hoyle et al., 2014). The reason is that these metrics often show poor proportionality because of a changing catchability as a result of the technical improvements over the whole exploitation history as well as unbalanced individual fishing characteristic of fishing vessels (Maunder and Punt, 2004; Maunder et al., 2006; Tidd et al., 2017). At a set scale, setting on free swimming schools (FSC) signifies the presence of tuna shoals, thus increasing their detectability; however, it is technologically and strategically demanding and usually makes the catch abortive or low yielding. As a consequence, it is interesting to discriminate habitat characteristics in comparative scenarios, comparing one scenario with nominal CPUE as an index of relative abundance and another scenario with the calibrated CPUE integrating the fishing characteristics to control local catchability.

Quantifying the habitat characteristics of skipjack tuna and the potential impacts of climate variability is a priority for fishery managers to develop effective advices under different climate scenarios and to contribute to sustainable tuna fisheries. For this purpose, the present study identified the habitat traits based on a series of oceanographic factors from the global ocean reanalysis model. Moreover, a comparison was conducted between two habitat models based on unprocessed purse seine CPUE and standardized CPUE by considering fishing characteristics. Finally, the impact of ENSO events on the abundance of skipjack tuna was examined in terms of the distribution and quality of the habitat.

2 Materials and methods

2.1 *Purse seine fishery-dependent data*

The fishery data used in this study originated from the log books of Chinese purse seine fleets from 2013 to 2017, which was provided by the National Data Center for Distant-water Fisheries of China. The fishing area was located in the western and central Pacific waters and spanned from 10°N to 10°S, and 140°E to 150°W, where the majority of global tuna catch has historically taken place. In this area, advection from the SEC entraining massive nutrient transports westward until the waters collide with the Warm Pool on the eastern edge, which induces a convergence zone with well-marked fronts (Fig. 1a). Complicated oceanographic phenomena in the region play a significant role and cause this area to be the most biologically productive region.

Fisheries data include daily geo-referenced fishing locations (i.e., latitude and longitude), catch in tons (separated into skipjack tuna and yellow fin tuna), fishing time (day), as well as specifications for each vessel. Only the portion of fishing sets targeting FSC of the skipjack tuna was used because this population, unlike fishing aggregating device (FAD)-associated school, allows to obtain the actual habitat for skipjack tuna under natural conditions. A total of 7 646 fishing sets were collected during the investigated period, around half (~3 387 fishing sets) of which represented positive catches.

The time frame of fishing operations covered a strong and prolonged El Niño episode, which lasted from the last two months of 2014 to the first four months of 2016. The mean SST anomalies in the Niño 3.4 region was consecutively above the threshold of positive 0.5°C (https://www.esrl.noaa.gov/psd/gcos_wgsp/Timeseries/Nino34/). A weak La Niña condition was identified in the last four months of 2017, while the remaining months were in an ENSO-neutral state. The spatial distribution of catches from 2013 to 2017 was presented by a kernel density contour in Fig. 1b. Regions in red represent the spatial locations of fish presence with high probability for FSC. The major fishing region was confined at the west of longitude 180° with two separated hot spots at 160°E and 170°E.

2.2 *Physical and biological environment*

Sea surface temperature (SST, °C), sea surface salinity (SSS), sea surface height above geoid (SSH, m), mixed layer thickness (MLT, m), eastward velocity (*u* component, m/s), and northward velocity (*v* component, m/s) of the sea surface current were obtained from Global Ocean Ensemble Reanalysis, which was pro-

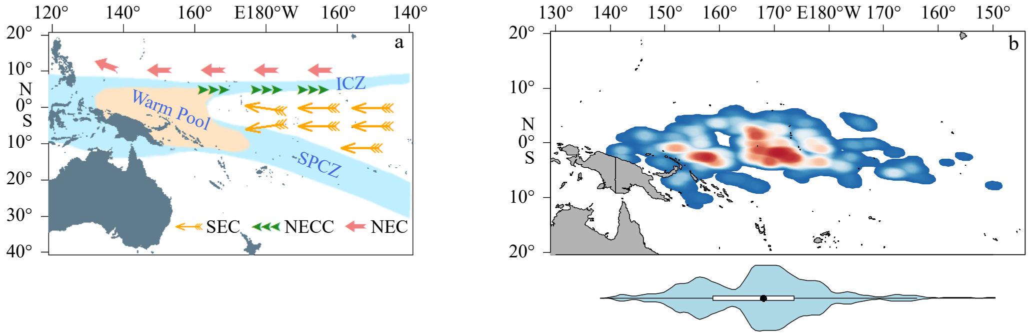

Fig. 1. Major oceanographic features in the fishing area of Pacific Ocean. a. SEC represents South Equatorial Current; NECC, North Equatorial Counter Current; NEC, North Counter Current; ICZ, Intertropical Convergence Zone; SPCZ, South Pacific Convergence Zone; b. kernel density contour of fish school presence in the fishing region from 2013 to 2017. High density regions are indicated in red in b. At the bottom of b, the zonal intensity of fish schools is indicated by a violin plot, representing the persistent thermal region around the 160°E and 170°E meridian.

duced with a numeric ocean model constrained with data assimilation of satellite and *in situ* observations. The system uses four model ensemble approaches (GLORYS2V4, ORAS5, GloSea5, and C-GLORS05) to estimate the 3-D gridded physical state of the ocean, covering the period of 1993–2018. The product was provided by the Copernicus Marine Environment Monitoring Service (CMEMS) with data at (1/4)° horizontal resolution, daily-mean temporal resolution, and 75 depth levels coverage (https://resources.marine.copernicus.eu/?option=com_csw&view=details&product_id=GLOBAL_REANALYSIS_PHY_001_031). In addition, given that the water layer occupied by skipjack tuna is usually located within the mixed layer, the temperatures at depth 50 m (T_{50}) and 100 m (T_{100}), as well as salinity levels at 50 m (S_{50}) and 100 m (S_{100}) were also used as sub-surface variables.

Sea surface chlorophyll *a* (SSC, mg/m^3) and dissolved oxygen (SSO, mL/L) were obtained from the biogeochemical hindcast for global oceans produced at Mercator-Ocean (Toulouse, France) and was also provided by the Copernicus Marine Environment Monitoring Service (CMEMS) (http://marine.copernicus.eu/services-portfolio/access-to-products/?option=com_csw&view=details&product_id=GLOBAL_REANALYSIS_BIO_001_029). It uses the PISCES biogeochemical model with initial conditions from World Ocean Atlas 2013. 3D biogeochemical fields provide daily-averaged data at (1/4)° horizontal resolution with 75 vertical levels. Also, we obtained the dissolved oxygen at multi-layers, i.e., 50 m (O_{50}), 61 m (O_{61}), 69 m (O_{69}), 77 m (O_{77}), 86 m (O_{86}), and 100 m (O_{100}). The skipjack tuna hypoxic depth (THD) was derived from the shallowest depth at which the dissolved oxygen concentration achieves approximately the threshold of 3.5 mL/L, which is considered to be the minimal requirement of oxygen for skipjack tuna (Barkley et al., 1978).

Sea surface current velocity (SSV, m/s) was calculated based on the eastward velocity (u) and northward velocity (v) as follows:

$$\mathrm{SSV} = \sqrt{u^2 + v^2}. \tag{1}$$

A gradient-based method was used to calculate the gradient value as the proxy of fronts of SST, SSS, and SSC, based on the following algorithm:

$$G_{i,j} = \sqrt{\left(\frac{S_{i+1,j} - S_{i-1,j}}{D_x}\right)^2 + \left(\frac{S_{i,j+1} - S_{i,j-1}}{D_y}\right)^2}, \tag{2}$$

where $G_{i,j}$ represents gradients (SST-grad, SSS-grad, and SSC-grad) at coordinate (i, j), $S_{i,j}$ represents the SST/SSS/SSC value at coordinate (i, j), D_x represents the geographical distance between locations (i+1, j) and (i-1, j), and D_y represents the geographical distance between locations (i, j+1) and (i, j-1).

In addition, the southern oscillation index (SOI) was downloaded as a quantitative index for monitoring climatic variability from the NOAA ESRL Physical Sciences Laboratory (https://psl.noaa.gov/gcos_wgsp/Timeseries/SOI/). A positive SOI indicates that the pressure in the Southeast Pacific is higher than in the western Pacific, representing the La Niña phenomenon, while a negative SOI represents the El Niño phenomenon.

2.3 *CPUE definition and standardization*

The purse seine nominal CPUE was defined as catch per fishing day. However, when the fishing operation for a certain vessel consecutively occurred on a fishing day and within short distance (e.g., one degree square), it was likely that the fishing sets were aimed at the same fish shoals. In such cases, the CPUE for these fishing sets was defined as the sum of the catch divided by one fishing day.

Purse seine catch is highly subject to the performance of both the vessel and the seine net. To better estimate the actual abundance, a generalized linear mixed model (GLMM) with Gaussian error distribution was employed to implement the standardization of raw CPUE. In the model, year, month, and spatial-grid data were treated as random effects to account for the non-homogeneous spatial and temporal distribution (Katara and Gaertner, 2014; Katara et al., 2017). For the spatial-grid data, we created topological structure over the entire fishing area by setting cell size to 1 degree square, in which the fishing locations were aggregated and a total of 1 583 cells were consecutively numbered. Explanatory variables of fixed effects include the vessel date of build (D), main engine power (P), total length of the vessel (L), and gross tonnage of vessel (T). These metrics were considered to be continuous and non-interactive, while the type of fishing gear (G, including knotted net and knotless net) and the type of FSC caught (S, including schools feeding on baitfish and non-associated school) were treated as categorical variables. Before standardization, we conducted the collinearity diagnostic for the variables D, P, L, T by computing the variance-inflation factor (VIF) in a generalized linear model. Variables with VIF exceeding 5 were removed from the model. Furthermore, the model only considered positive catch records to avoid the influence from completely skulled set (i.e., zero catch) and random effects only reacted on the intercept.

Finally, standardized CPUE were predicted by producing the least squares mean for random effects to eliminate the influence of fishing capability. Fits for GLMM were performed in R (version 3.3.0) with the lme4 package. Linear estimates were chosen based on the restricted maximum likelihood (REML) criterion. An automatic backward elimination procedure was adopted to non-significant terms based on Sattethwaite's approximation for fixed effects and likelihood ratio test for random effects using R (version 3.3.0) with the lmerTest package.

2.4 *Habitat analysis*

The difference of habitat characteristics was derived from analysis based on unprocessed CPUE and standardized CPUE as a proxy of population abundance. A generalized additive model (GAM) with lognormal error distribution was used to model non-linear relationships between the relative index of abundance and independent environmental variable at a daily resolution (Arrizabalaga et al., 2015; Lopez et al., 2017). The explanatory variables incorporate abiotic factors (SST, SSS, SSH, SSV, SSO, MLT, THD, T_{50}, T_{100}, S_{50}, S_{100}, O_{50}, O_{61}, O_{69}, O_{77}, O_{86}, O_{100}, SST-grad, and SSS-grad), biotical factors (SSC and SSC-grad), and the climatic factor (SOI), of which THD was treated as the categorical variable. All continuous variables were modelled by spline functions of four smoothness degrees to avoid over-fitting. Prior to modelling, we conducted the collinearity diagnostic for continuous variables by computing VIF in a generalized linear model. Variables with VIF more than five were removed from the model.

Model selection was evaluated by considering the significance of the terms, deviance explained, and the Akaike Information Criterion (AIC) value based on a backward elimination of all effects. GAM regressions were built in R (version 3.3.0) with the MGCV package.

2.5 *Habitat quantification and variations under ENSO events*

The optimal model was used to output the predicted CPUE based on the actual daily value of significant variables. The habitat quantification process simply used the predicted CPUE divided by the maximum predicted CPUE for the cells to obtain the habitat suitable index (HSI) at a scale of 0 to 1 (Tian et al., 2009; Yu and Chen, 2021). Three typical fishing days (January 1, 2013; August 1, 2015; and January 1, 2017), representative of La Niña, El Niño, and neutral conditions, respectively, were selected to identify differences of habitat distribution in two scenarios of habitat modelling based on CPUE.

To examine the consequences of climate variability on the habitat quality of skipjack tuna, the monthly averaged HSI we computed for all cells in the time series of 2013 to 2017. A linear model between HSI and SOI was fitted to determine whether the ENSO events are significantly correlated with the habitat of skipjack tuna.

3 Results

3.1 *Calibration of nominal CPUE*

VIFs for the variables *P* (5.04), *L* (7.5), and *T* (10.6), showed strong collinearities with *D* (1.8). The mixed model for calibration of nominal CPUE indicates that the random effect terms year (*Y*) and spatial-grid data are significant (p<0.05), while the term month (*M*) has no significant effect (p=1). For these terms of fixed effect, all variables (*D*, *G*, and *S*) are significant at the 0.05 level (Table 1).

Table 1. Summary for the significant covariates as fixed effect in the optimal model of CPUE standardization

Covariates as fixed effect	Estimate value	SD	*t* statistics	*p*	AIC
D	0.40	0.10	3.94	<0.05	
G (factor 2)	11.07	4.15	2.67	<0.05	33 756
S (factor 2)	–4.79	2.18	–2.2	<0.05	

Note: SD represents standard error; *D*, the vessel date of build; *G*, the type of fishing gear; *S*, the type of free swimming schools caught; AIC, the Akaike Information Criterion.

As shown in Fig. 2, positive intercept estimates appear in the years of 2015 (4.51) and 2016 (3.09), suggesting that years that experiencing significant El Niño periods positively affect catch, while the minimum intercept estimate was found in 2017 (–4.92), when the last four months experienced a weak La Niña condition. Vessel date of build has a positive slope on CPUE in the linear estimate, suggesting that CPUE are higher for relatively new vessels. Moreover, the use of knotless nets (factor 2 of *G*), compared with knotted nets (factor 1), has higher CPUE. Setting on free-swimming school (factor 2 of *S*) caught fewer fish than setting on school feeding on baitfish (factor 1). Spatial effect showed that the high random intercepts are, to a great extent, scattered over the entire fishing areas, suggesting high variation of geographical distribution for high CPUE under climatic variability. Model backward elimination and diagnostic-plots (slope, residuals, and model assumption checks) are shown in Table S1 and Figs S1–3.

3.2 *Comparison of habitat models using different CPUEs*

VIFs for environment variables O_{50} (31.8), O_{61} (193.7), O_{69} (392.1), O_{77} (476.3), O_{86} (338.6), and O_{100} (67.9), that have strong collinearities with SSO (1.8), were removed from the model. The optimal model based on nominal CPUE only explains 2.6% deviance, and only includes significant variables T_{100}, S_{50}, S_{100}, and SOI (Table 2). In comparison, the optimal model based on calibrated CPUE has much higher deviance explained (35%) and included most of the variables in the full model except for the insignificant terms MLT, S_{100}, SST-grad, and THD (see backward model selection in Table S2 and model diagnostic-plots in Fig. S4).

Habitat models indicate contrasting HSI distribution between the use of nominal CPUE (Fig. 3a) and calibrated CPUE (Fig. 3b). Under typical La Niña (January 1, 2013) and neutral (January 1, 2017) conditions, scenario A shows a similar geographic distribution of high-quality habitat in the west of longitude 180° at south latitudes and the east of longitude 180° at north latitudes. Along the equator very low HIS was found. Under El Niño conditions (August 1, 2015), the quality and size of the habitat increased at the west and east, despite its still low HSI around equatorial waters east of 160°E. In comparison, scenario B shows high HSI in the west of 160°E on January 1, 2013 and in the east of 160°E on January 1, 2017. Under El Niño conditions (August 1, 2015), the quality and size of the habitat improve and expand to east of longitude 180°. Overlaid catches show rough concurrence with the hotspot of HSI predicted by the model using calibrated CPUE. This indicates the superiority of this method over model A which fails in the validation especially under the neutral condition (January 1, 2017).

3.3 *Habitat characteristics and consequence under ENSO variability*

Figure 4 shows the partial effect of individual explanatory variable from scenario B to characterize the habitat of skipjack tuna. Temperature-related factors interpret the monotone rela-

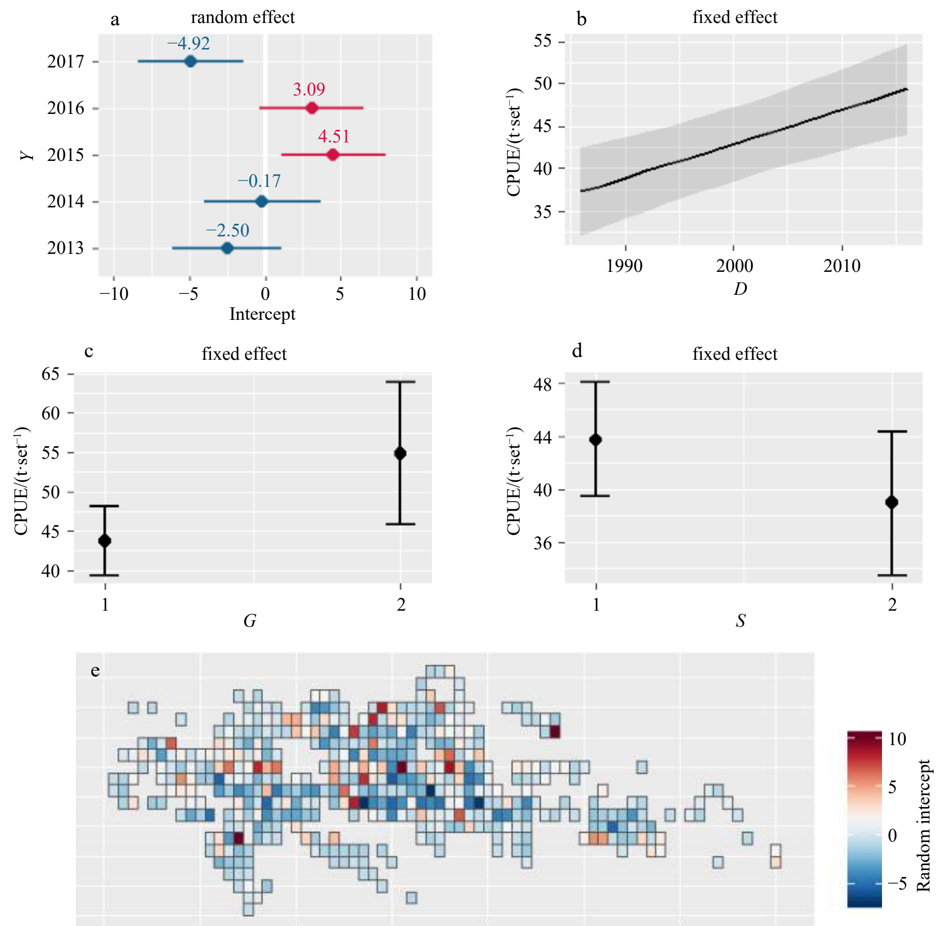

Fig. 2. Linear estimates of GLMM for random effect terms year (*Y*) on intercept (a) and a range of fixed effects (the vessel date of build, *D*; the type of fishing gear, *G*; and the type of free swimming schools caught, *S*) (b, c and d). a. Positive coefficients (in red) indicate positive effects on CPUE, whereas negative effects indicate minus coefficients (in blue). In a–d, bars and shaded region indicate 95% confidence intervals. e. The random intercepts of spatial-grid are mapped onto the corresponding fishing cells (1 degree square). For the purpose of protecting the commercial confidentiality, position information is not labelled aside the axis.

Table 2. Summary for the significant covariates in the optimal habitat models under scenarios of using nominal CPUE and calibrated CPUE

	Habitat models							
	Based on nominal CPUE				Based on calibrated CPUE			
AIC score	33 738				18 129			
Adjusted R^2	0.023				0.35			
Deviance explained	0.026				0.35			
	Variable	EDF	F	p	Variable	EDF	F	p
	T_{100}	1.48	7.29	<0.05	SST	2.83	6.49	<0.05
	S_{50}	2.78	2.71	<0.05	T_{50}	2.17	6.45	<0.05
	S_{100}	2.71	3.61	<0.05	T_{100}	2.90	41.33	<0.05
	SOI	1.00	9.67	<0.05	SSS	2.85	29.48	<0.05
					S_{50}	2.99	21.08	<0.05
					SSH	2.84	29.53	<0.05
					SSV	2.86	7.04	<0.05
					SSC	2.84	5.38	<0.05
					SSO	2.94	23.78	<0.05
					SSS-grad	2.10	5.21	<0.05
					SSC-grad	1.00	46.09	<0.05
					SOI	2.84	96.09	<0.05

Note: EDF represents estimated degree of freedom; *F* represents *F* statistics.

tionship with CPUE. Fish prefer warmer SST within the incredible range of 28°C to 31°C, while CPUE increased with decreased temperature at 50 m and 100 m. SSS and sub-surface salinity at 34.8 and 34.5, respectively, have the maximum effect on CPUE.

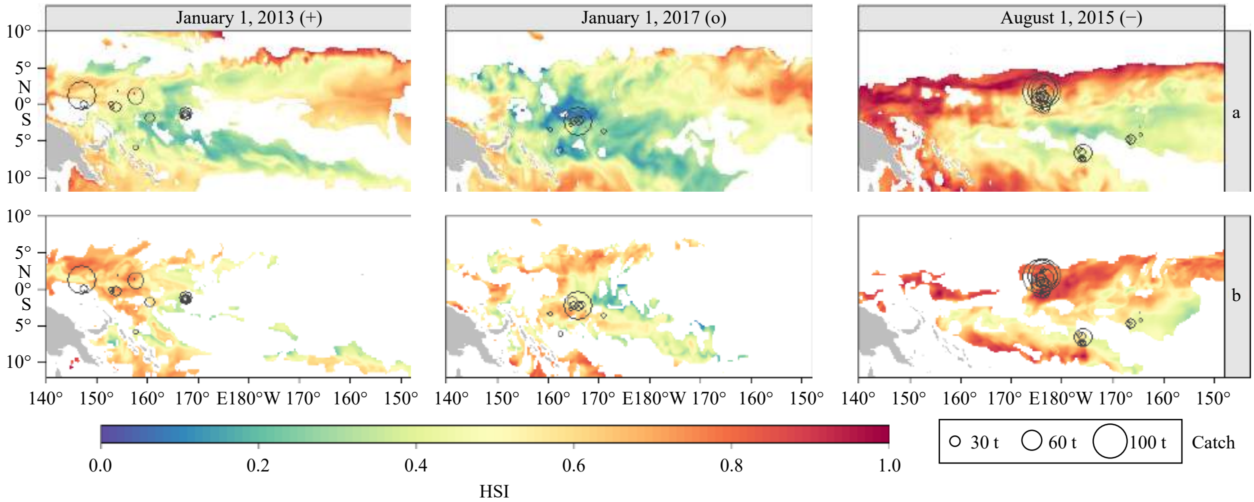

Fig. 3. HSI distribution between models using nominal CPUE (a) and calibrated CPUE (b) on January 1, 2013, January 1, 2017 and August 1, 2015. ENSO periods are denoted by "+": La Niña; "–": strong El Niño; "o": neutral condition. White regions indicate the null HSI due to the environmental data beyond the range of model prediction or at incredible interval. Open circles indicate catches in the corresponding month rather than day when fishing efforts are scarce.

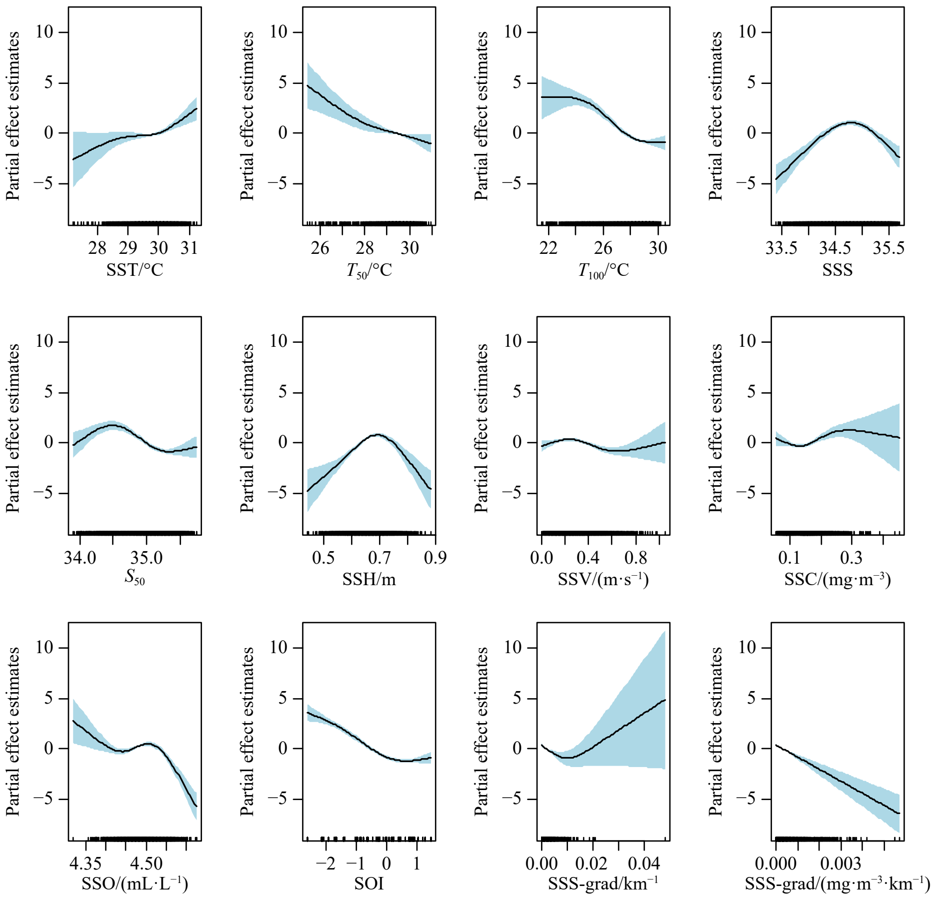

Fig. 4. Partial effect estimates of GAM for significant variables. Blue-shaded regions are 95% confidence bands for smooths. Density of raw data is displayed as a rug at the foot of each plot.

The most preferred SSH of skipjack is 0.7 m based on maximum partial effect. The partial effect curves of SSV and SSC are relatively flat, suggesting that the variation has little effects. The monotonic decreasing trend of SOI suggests that CPUE increases during under El Niño conditions and decreases under La Niña conditions. SSS-grad and SSC-grad shows negative relationship with CPUE over an incredible interval, although an abnormally high value of SSS-grad indicates the maximum partial effect estimate.

Monthly averaged HSI showed a significant linear relationship with SOI at R^2=0.76 (Fig. 5). During El Niño episodes, the averaged HSI have values exceeding 0.4, while most of them remain below 0.4 during La Niña episodes. This indicates that El Niño episodes eventually provide more preferable habitat for skipjack tuna under ENSO variability.

4 Discussion

Fish living in pelagic habitats neither occupy ocean spaces randomly nor homogeneously (Tew Kai and Marsac, 2010; Lopez et al., 2017). It is generally accepted that an attractive dwelling site or habitat hot-spot is identified by dynamic marine physical chemistry processes and active trophic interactions. At a global scale, productive tuna habitats depend on localized monsoon and currents system to dominate the seasonal migration of tuna for feeding. For instance, a transition zone bounded by two fronts of confluence of the warm Kuroshio Current and the cold Oyashio Current in the western North Pacific Ocean (Nihira, 1996; Zainuddin et al., 2008; Mugo et al., 2010), a semi-permanent coastal upwelling generated by both the Ekman transport and the Asian monsoon in the eastern Indian Ocean (Setiawati et al., 2015; Zainuddin et al., 2017), subtropical convergence of the Southwest Atlantic (Andrade and Garcia, 1999; Andrade, 2003), and coastal fronts caused by boundary current upwelling in the Northeast Pacific Ocean (Laurs and Lynn, 1977; Phillips et al., 2014). The perspective of the present study focuses on localized territory, a patch of persistently active area of tuna purse seine fishing in the western and central Pacific Ocean. Oceanic traits allow for the development of distinctive interests of skipjack tuna to utilize this unique physical environment and ecosystem. This strong dependency on a particular set of environmental structures results in the reliable prediction of highly productive fishing grounds. Additionally, the timeframe of the present study covers a strong El Niño event from 2014 to 2016 and a weak La Niña event in 2017. This provides situation in the context of climate variability that allowed for a demonstration of the tight adherence if skipjack tuna to habitat preferences, and eventually, enable this interpretation of the habitat variability driven by environmental change. Purse seine fishing fleets targeting FSC harvest mixed surface-inhabiting tuna species, primarily composed of skipjack tuna. Although this species seasonally expands its geographical distribution into temperate waters both northward and southward along warm currents through feeding migration, skipjack tuna tend to make small movements within their home range to locate regions with suitable habitat (Dueri et al., 2014). This region was selected since the unique ecosystem and warm waters reflects the habitat trait of tuna. Broadly, the results of this study support the assertion that the development in the quality and size of the favorable habitat is the potential reason of increased abundance of skipjack tuna during El Niño episodes.

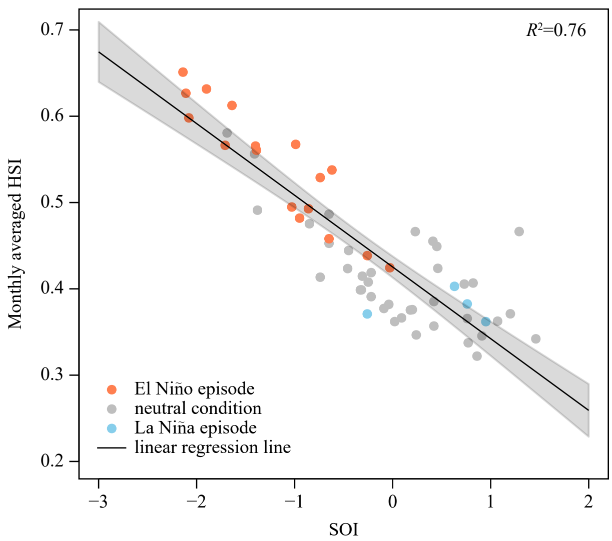

Fig. 5. Linear relationship between monthly averaged HSI and SOI. Red, gray, and blue dots indicate El Niño episode (defined as six-consecutive-month average sea surface temperature anomaly exceeding 0.5°C), neutral condition, and La Niña episode (defined as six-consecutive-month average sea surface temperature anomaly less than negative 0.5°C), respectively. Shaded regions indicates 95% confidence band.

Tuna purse seine fishery data involves multiple set categories. It is therefore necessary to make this distinction because of different habitat choices as a consequence of potential behavior diversity between FSC and associated schools. The present study focuses on free swimming schools and is complementary to the study of Lopez et al. (2017), who ascertained the drifting FAD (DFAD) associated fish aggregations and their environment preference by using large-scale remote sampling. The data they used were obtained from echo sounder buoys and served as an effective index to describe fish presence/absence and biomass density. In contrast, fishery data has been criticized for their biased estimates on stock abundance (Maunder and Punt, 2004; Maunder et al., 2006). This bias is more likely exaggerated in the case of free school sets, because catch volumes are extremely sensitive to fishing practices. Based on previous research, the selection of the relative abundance index remains controversial. Either fishing efforts (Yen et al., 2017) or catchs (Wang et al., 2014) have been used to substitute for catch/effort in purse seine fisheries. However, the present study used a defined nominal CPUE where the catches are pooled when multiple fishing sets in a fishing day and fishing cell by the same vessel were detected. This approach could eliminate cases where CPUE may be underestimated when several fishing efforts are consecutively directed on the same school.

Previous habitat models commonly directly fit the raw CPUE with environmental variables, particularly using pole-and-line or longline fisheries data (Mugo et al., 2010; Yen et al., 2017); alternatively, the standardized CPUE was used despite the inclusion of only temporal and spatial effects in the model (Lan et al., 2018). The present study found that the scenario of using standardized CPUE, which considers fishing characteristics, could model the regular zonal shift of habitat compatible with the observed fishing efforts transfer. This model showed better prediction capacity than a scenario that used unprocessed CPUE.

CPUE as indices of abundance for stock assessment indices mainly concerns factors that affect local catchability, and environmental variables should not be included in the standardization model as explained factors, since they are not captured by the time effect (Hoyle et al., 2014). In the habitat model, however, it was assumed that the environment factors are already included in the spatial and temporal information in the first CPUE standardization process and are separately captured in the following step. However, this study also acknowledged that the model has uncertain reliability due to the process error in the two serial stages. Also, a number of environmental factors affect both the fish abundance and catchability in different ways. For example, the shoaling and deepening of MLT and THD, as well as the magnitude of SSV may significantly affect the success of a catch.

The GLMM used for CPUE standardization offers the advantage of accounting for both spatial and temporal heterogeneity by treating these parameters as random effects (the same approach was applied by Katara and Gaertner (2014)). The effect of *Y* shows a beneficial influence on catch rates in those years of the El Niño period (from 2014 to 2016), which might be the result of a relatively shallow surface-mixed layer. The climatic change in turn increases the catchability of the species in purse seine fishery. For the fixed linear effects, using knotless nets increased catches compared with the use of knotted nets. Indeed, because of their superior hydrodynamic performance, knotless nets can be favorable for rapid sinking and improved fishing efficiency (Zhou et al., 2015). Another significant term is the type of non-associated school, which suggests that fishing sets on those fish feeding on baitfish would achieve higher catch rates. It seems reasonable to assume that schools feeding on baitfish compared with free-swimming fish might stay more steadily on the surface layer, resulting in a higher vulnerability to fishing gear.

Among these significant variables associated with habitat, SSS presents unimodal function within the credible range. Skipjack tuna likely formed high abundance at moderate sea surface salinity of ~34.8. This result corroborates the results of Yen et al. (2017), who reported an optimal SSS value (34.7) as the most favorable habitat for skipjack tuna in the western and central Pacific Ocean. However, these findings contrast with the results reported by Arrizabalaga et al. (2015), who reported a relatively higher salinity preference at ~36–37. This could be because they used extensive longline datasets across all oceans, with the notable exception of the western and central Pacific. Skipjack tuna exhibit a poleward distribution in colder and saltier waters. However, the deduction of salinity affecting the geographical distribution and abundance of populations through physiology or processes of oceanic physics seems to be untenable, since such small changes in salinity cannot be detected by skipjack tuna. Skipjack tuna are more likely attracted by the oceanic features associated with color and temperature, which correlated with salinity in the spatial distribution.

Skipjack tuna are observed in the region of restricted SST range with no more than 3°C (28°C to 31°C), which agrees with the highest CPUE areas in the western equatorial Pacific (Zainuddin et al., 2017). However, the conclusions of the present study indicate slightly warmer and narrower range than the currently accepted SST range (24°C to 28°C) for DFAD-associated tuna data in the Atlantic Ocean (Lopez et al., 2017). A plausible explanation could be attributed to the ecological effect of FADs, or to the differences between FSC and FAD-associated schools. In general, the obtained result indicates that skipjack tuna always prefer of relatively higher SST and lower temperature in the subsurface water. This suggests that the abundance of fish would likely increase in waters with shallower mixed layer thickness. Cold waters lading rich macronutrients represented good feeding opportunities and in cold, high productivity waters, skipjack tuna are able to exploit patches of food resources (Kirby et al., 2000). It is possible that skipjack tuna would benefit from the shoaling of the stratification boundary, which increases prey accessibility and decreases energy costs for diving in cold water to forage. Also, this is likely just a reflection of higher catchability in cases where shoaling of thermocline depth compresses the vertical distribution of fish which increases the catch rate.

Skipjack tuna inhabit the upper zone of pelagic environments, which are generally considered to be prey-scarce environments. Promoted productivity will lead to an accumulation of prey organisms, which determined the abundance and distribution of tuna. The SSC was hence a proxy of food enrichment, as the source of energy circulating to connect trophic levels. The importance of the SSC in the model was emphasized by a high explained deviance. Skipjack tuna were abundant where SSC value was low, which differed from the findings of Zainuddin et al. (2017). They reported that persistent habitat hotspots could be identified by the presence of 0.2 mg/m^3 SSC isopleth. This might be due to focus on different study regions, e.g. the present study focused on the pelagic ocean compared to their region near land, which generally has higher SSC. Indeed, SSC was not the direct predictor of high tuna abundance, but rather, large aggregations of plankton benefiting from the downstream development of high productivity (Lehodey et al., 1997). This phenomenon has been well supported by the increasing concentration of tuna schools at least 9 d after phytoplankton blooms (Fonteneau et al., 2008). The diet of tuna primarily consists of lower trophic level micronekton that ensures SSC as a biotic factor pertinent to tuna abundance. However, the nutritive process of tuna is dynamically complicated. Therefore, the inclusion of field prey information improves predictions of their distribution and refines the current understanding of their behaviors (Polovina et al., 2001; Schick and Lutcavage, 2009; Mugo et al., 2014). It is well established that oceanic fronts are intimately linked to the congregation of plankton and micronekton, and thus sustain high biological density. However, using the two terms associated with physical and biological environment gradients (SSS-grad and SSC-grad) as the proxy of fronts in the present study, exerted negative partial effects on the abundance. In fact, due to the fine scale of environmental data, based on the utilized approach, the calculated gradients do not necessarily represent the magnitude of fronts. Consequently, the detection of fronts in the spatial distribution based on image processing as well as the implement of establishing their relationship with abundance should be investigated in a further study.

Although mixed layer thickness in the model could not prove the contribution to the variation of CPUE, it can still be speculated that the changing stratification of the upper ocean is responsible for the habitat variability under ENSO events. Shallower surface mixed layer and the shoaling of thermocline as the major process during El Niño are assumed to be related to increased catchability. These also decrease the range of depth used by skipjack tuna and increase the density/abundance of fish (Yen et al., 2017). Moreover, as a side effect, thermocline shoaling could raise macronutrients into the photic zone and increased primary production (Matear et al., 2015). Previous studies have emphasized the influence of climatic fluctuations on the spatial dynamics processes, e.g., mortality, reproduction, and recruitment (Lehodey et al., 1997; Lehodey et al., 2008; Lima and Naya, 2011). During El Niño years, the expansion experienced by the warm pool and the subsequent enlargement of the spawning grounds appear to benefit the recruitment processes of skipjack tuna (Lehodey et al., 2003). However, the enrichment in zooplankton of the western Pacific is highly favorable for both survival and larval development of tuna (Lehodey, 2001). From the perspective of the ecological habitat, the results of the present study consolidate the inference of the significant effect from ENSO events based on a quantitative statistics framework, and may be compatible and complementary to the spatial population dynamics model (e.g., SEPODYM). El Niño episodes positively impact the habitat in quantitative and qualitative terms, which is the main cause of an increased abundance of skipjack tuna.

References

Andrade H A. 2003. The relationship between the skipjack tuna (*Kat-*

suwonus pelamis) fishery and seasonal temperature variability in the south-western Atlantic. Fisheries Oceanography, 12(1): 10–18, doi: 10.1046/j.1365-2419.2003.00220.x

Andrade H A, Garcia C A E. 1999. Skipjack tuna fishery in relation to sea surface temperature off the southern Brazilian coast. Fisheries Oceanography, 8(4): 245–254, doi: 10.1046/j.1365-2419.1999.00107.x

Arrizabalaga H, Dufour F, Kell L, et al. 2015. Global habitat preferences of commercially valuable tuna. Deep-Sea Research Part II: Topical Studies in Oceanography, 113: 102–112, doi: 10.1016/j.dsr2.2014.07.001

Barkley R A, Neill W H, Gooding R M. 1978. Skipjack tuna, *Katsuwonus pelamis*, habitat based on temperature and oxygen requirements. Fishery Bulletin, 76(3): 653–662

Bernal D, Brill R W, Dickson K A, et al. 2017. Sharing the water column: physiological mechanisms underlying species-specific habitat use in tunas. Reviews in Fish Biology and Fisheries, 27(4): 843–880, doi: 10.1007/s11160-017-9497-7

Bertignac M, Lehodey P, Hampton J. 1998. A spatial population dynamics simulation model of tropical tunas using a habitat index based on environmental parameters. Fisheries Oceanography, 7(3–4): 326–334, doi: 10.1046/j.1365-2419.1998.00065.x

Brill R W. 1994. A review of temperature and oxygen tolerance studies of tunas pertinent to fisheries oceanography, movement models and stock assessments. Fisheries Oceanography, 3(3): 204–216, doi: 10.1111/j.1365-2419.1994.tb00098.x

Dueri S, Bopp L, Maury O. 2014. Projecting the impacts of climate change on skipjack tuna abundance and spatial distribution. Global Change Biology, 20(3): 742–753, doi: 10.1111/gcb.12460

Fonteneau A, Lucas V, Tewkai E, et al. 2008. Mesoscale exploitation of a major tuna concentration in the Indian Ocean. Aquatic Living Resources, 21(2): 109–121, doi: 10.1051/alr:2008028

Hoyle S D, Langley A D, Campbell R A. 2014. Recommended approaches for standardizing CPUE data from pelagic fisheries. Kolonia, Pohnpei State, Federated States of Micronesia: WCPFC Scientific Committee, https://meetings.wcpfc.int/index.php/node/8709[2014-7-1/2019-9-1]

Katara I, Gaertner D. 2014. Some news approaches for standardizing tropical purse seiners CPUEs. Victoria Mahé, Seychelles: IOTC Working Party on Tropical Tunas, https://www.iotc.org/sites/default/files/documents/2014/11/IOTC-2014-WPTT16-16_-_PS_CPUE_Standardisations.pdf[2014-11-12/2019-7-10]

Katara I, Gaertner D, Billet N, et al. 2017. Standardisation of skipjack tuna CPUE for the EU purse seine fleet operating in the Indian Ocean. Victoria Mahé, Seychelles: IOTC Working Party on Tropical Tunas, https://www.iotc.org/sites/default/files/documents/2017/10/IOTC-2017-WPTT19-38_SKJ_EU_PS_CPUE.pdf [2017-10-6/2019-12-4]

Kirby D S, Fiksen Ø, Hart P J B. 2000. A dynamic optimisation model for the behaviour of tunas at ocean fronts. Fisheries Oceanography, 9(4): 328–342, doi: 10.1046/j.1365-2419.2000.00144.x

Lan K W, Lee M A, Chou C P, et al. 2018. Association between the interannual variation in the oceanic environment and catch rates of bigeye tuna (*Thunnus obesus*) in the Atlantic Ocean. Fisheries Oceanography, 27(5): 395–407, doi: 10.1111/fog.12259

Laurs R M, Lynn R J. 1977. Seasonal migration of North Pacific albacore, *Thunnus alalunga*, into North American coastal waters: distribution, relative abundance, and association with transition zone waters. Fishery Bulletin, 75(4): 795–822

Le Borgne R, Barber R T, Delcroix T, et al. 2002. Pacific warm pool and divergence: temporal and zonal variations on the equator and their effects on the biological pump. Deep-Sea Research Part II: Topical Studies in Oceanography, 49(13–14): 2471–2512, doi: 10.1016/S0967-0645(02)00045-0

Lehodey P. 2001. The pelagic ecosystem of the tropical Pacific Ocean: dynamic spatial modelling and biological consequences of ENSO. Progress in Oceanography, 49(1–4): 439–468, doi: 10.1016/S0079-6611(01)00035-0

Lehodey P, Bertignac M, Hampton J, et al. 1997. El Niño Southern Oscillation and tuna in the western Pacific. Nature, 389(6652): 715–718, doi: 10.1038/39575

Lehodey P, Chai Fei, Hampton J. 2003. Modelling climate-related variability of tuna populations from a coupled ocean-biogeochemical-populations dynamics model. Fisheries Oceanography, 12(4–5): 483–494, doi: 10.1046/j.1365-2419.2003.00244.x

Lehodey P, Senina I, Calmettes B, et al. 2013. Modelling the impact of climate change on Pacific skipjack tuna population and fisheries. Climatic Change, 119(1): 95–109, doi: 10.1007/s10584-012-0595-1

Lehodey P, Senina I, Murtugudde R. 2008. A spatial ecosystem and populations dynamics model (SEAPODYM)—Modeling of tuna and tuna-like populations. Progress in Oceanography, 78(4): 304–318, doi: 10.1016/j.pocean.2008.06.004

Lima M, Naya D E. 2011. Large-scale climatic variability affects the dynamics of tropical skipjack tuna in the western Pacific Ocean. Ecography, 34(4): 597–605, doi: 10.1111/j.1600-0587.2010.06422.x

Lopez J, Moreno G, Lennert-Cody C, et al. 2017. Environmental preferences of tuna and non-tuna species associated with drifting fish aggregating devices (DFADs) in the Atlantic Ocean, ascertained through fishers' echo-sounder buoys. Deep-Sea Research Part II: Topical Studies in Oceanography, 140: 127–138, doi: 10.1016/j.dsr2.2017.02.007

Loukos H, Monfray P, Bopp L, et al. 2003. Potential changes in skipjack tuna (*Katsuwonus pelamis*) habitat from a global warming scenario: modelling approach and preliminary results. Fisheries Oceanography, 12(4–5): 474–482, doi: 10.1046/j.1365-2419.2003.00241.x

Matear R J, Chamberlain M A, Sun C, et al. 2015. Climate change projection for the western tropical Pacific Ocean using a high-resolution ocean model: Implications for tuna fisheries. Deep-Sea Research Part II: Topical Studies in Oceanography, 113: 22–46, doi: 10.1016/j.dsr2.2014.07.003

Maunder M N, Punt A E. 2004. Standardizing catch and effort data: a review of recent approaches. Fisheries Research, 70(2–3): 141–159, doi: 10.1016/j.fishres.2004.08.002

Maunder M N, Sibert J R, Fonteneau A, et al. 2006. Interpreting catch per unit effort data to assess the status of individual stocks and communities. ICES Journal of Marine Science, 63(8): 1373–1385, doi: 10.1016/j.icesjms.2006.05.008

Mugo R, Saitoh S I, Nihira A, et al. 2010. Habitat characteristics of skipjack tuna (*Katsuwonus pelamis*) in the western North Pacific: a remote sensing perspective. Fisheries Oceanography, 19(5): 382–396, doi: 10.1111/j.1365-2419.2010.00552.x

Mugo R M, Saitoh S I, Takahashi F, et al. 2014. Evaluating the role of fronts in habitat overlaps between cold and warm water species in the western North Pacific: a proof of concept. Deep-Sea Research Part II: Topical Studies in Oceanography, 107: 29–39, doi: 10.1016/j.dsr2.2013.11.005

Nihira A. 1996. Studies on the behavioral ecology and physiology of migratory fish schools of skipjack tuna (*Katsuwonus pelamis*) in the oceanic frontal area. Bulletin of Tohoku National Fisheries Research Institute (in Japanese), 58: 137–233

Phillips A J, Ciannelli L, Brodeur R D, et al. 2014. Spatio-temporal associations of albacore CPUEs in the northeastern Pacific with regional SST and climate environmental variables. ICES Journal of Marine Science, 71(7): 1717–1727, doi: 10.1093/icesjms/fst238

Picaut J, Ioualalen M, Menkes C, et al. 1996. Mechanism of the zonal displacements of the Pacific Warm Pool: implications for ENSO. Science, 274(5292): 1486–1489, doi: 10.1126/science.274.5292.1486

Polovina J J, Howell E, Kobayashi D R, et al. 2001. The transition zone chlorophyll front, a dynamic global feature defining migration and forage habitat for marine resources. Progress in Oceanography, 49(1–4): 469–483, doi: 10.1016/S0079-6611(01)00036-2

Roger C. 1994. Relationships among yellowfin and skipjack tuna, their prey-fish and plankton in the tropical western Indian Ocean. Fisheries Oceanography, 3(2): 133–141, doi: 10.1111/j.1365-2419.1994.tb00055.x

Schaefer K M, Fuller D W. 2007. Vertical movement patterns of skipjack tuna (*Katsuwonus pelamis*) in the eastern equatorial Pacific Ocean, as revealed with archival tags. Fishery Bulletin, 105(3): 379–389, doi: 10.1016/j.fishres.2007.01.005

Schick R S, Lutcavage M E. 2009. Inclusion of prey data improves prediction of bluefin tuna (*Thunnus thynnus*) distribution. Fisheries Oceanography, 18(1): 77–81, doi: 10.1111/j.1365-2419.2008.00499.x

Setiawati M D, Sambah A B, Miura F, et al. 2015. Characterization of bigeye tuna habitat in the Southern Waters off Java-Bali using remote sensing data. Advances in Space Research, 55(2): 732–746, doi: 10.1016/j.asr.2014.10.007

Tew Kai E, Marsac F. 2010. Influence of mesoscale eddies on spatial structuring of top predators' communities in the Mozambique Channel. Progress in Oceanography, 86(1–2): 214–223, doi: 10.1016/j.pocean.2010.04.010

Tian Siquan, Chen Xinjun, Chen Yong, et al. 2009. Evaluating habitat suitability indices derived from CPUE and fishing effort data for *Ommatrephes bratramii* in the northwestern Pacific Ocean. Fisheries Research, 95(2–3): 181–188, doi: 10.1016/j.fishres.2008.08.012

Tidd A, Brouwer S, Pilling G. 2017. Shooting fish in a barrel? Assessing fisher-driven changes in catchability within tropical tuna purse seine fleets. Fish and Fisheries, 18(5): 808–820, doi: 10.1111/faf.12207

Wang Xuefang, Chen Yong, Truesdell S, et al. 2014. The large-scale deployment of fish aggregation devices alters environmentally-based migratory behavior of skipjack tuna in the western Pacific Ocean. PLoS ONE, 9(5): e98226, doi: 10.1371/journal.pone.0098226

Yen K W, Wang G H, Lu H J. 2017. Evaluating habitat suitability and relative abundance of skipjack (*Katsuwonus pelamis*) in the western and central Pacific during various El Niño events. Ocean & Coastal Management, 139: 153–160, doi: 10.1016/j.ocecoaman.2017.02.011

Yu Wei, Chen Xinjun. 2021. Habitat suitability response to sea-level height changes: Implications for Ommastrephid squid conservation and management. Aquaculture and Fisheries, 6(3): 309–320, doi: 10.1016/j.aaf.2020.06.001

Zainuddin M, Farhum A, Safruddin S, et al. 2017. Detection of pelagic habitat hotspots for skipjack tuna in the Gulf of Bone-Flores Sea, southwestern Coral Triangle tuna, Indonesia. PLoS ONE, 12(10): e0185601, doi: 10.1371/journal.pone.0185601

Zainuddin M, Kiyofuji H, Saitoh K, et al. 2006. Using multi-sensor satellite remote sensing and catch data to detect ocean hot spots for albacore (*Thunnus alalunga*) in the northwestern North Pacific. Deep-Sea Research Part II: Topical Studies in Oceanography, 53(3–4): 419–431, doi: 10.1016/j.dsr2.2006.01.007

Zainuddin M, Saitoh K, Saitoh S I. 2008. Albacore (*Thunnus alalunga*) fishing ground in relation to oceanographic conditions in the western North Pacific Ocean using remotely sensed satellite data. Fisheries Oceanography, 17(2): 61–73, doi: 10.1111/j.1365-2419.2008.00461.x

Zhou Cheng, Xu Liuxiong, Hu Fuxiang, et al. 2015. Hydrodynamic characteristics of knotless nylon netting normal to free stream and effect of inclination. Ocean Engineering, 110: 89–97, doi: 10.1016/j.oceaneng.2015.09.043

Supplementary information:

Fig. S1. Diagnostic-plots for CPUE calibration model showing the slope of coefficients for each single predictor against the response (left) and against the residuals (right).

Fig. S2. QQ plot (left) and density plot (right) for checking for normal distribution of residuals of CPUE calibration model.

Fig. S3. Scatter plot for checking for homoscedasticity of CPUE calibration model.

Fig. S4. Diagnostic-plots for habitat model based on calibrated CPUE.

Table. S1. Backward selection with variables sequentially removed from habitat model based on nominal CPUE.

Table. S2. Backward selection with variables sequentially removed from habitat model based on calibrated CPUE.

The supplementary information is available online at https://doi.org/10.1007/s13131-021-1922-z and www.aosocean.com. The supplementary information is published as submitted, without typesetting or editing. The responsibility for scientific accuracy and content remains entirely with the authors.